JOURNAL OF THE CANADIAN SOCIETY OF EXPLORATION GEOPHYSICISTS
VOL. 21, NO. 1 (DEC. 1985), P. 89-97

MODELLING MARINE SEISMIC ACQUISITION SYSTEMS IN THE kf DOMAIN[1]

PETER M. DUNCAN[2]

ABSTRACT

Modelling and measurement of the far field signature of airgun arrays have been used for some time now to design a better marine seismic source. In this paper the presentation of the array signature is made in the Fourier (kf) domain. This allows for the inclusion of source and receiver ghosts and source and receiver group response. As a result, a total system response is derived. The presentation in this fashion not only lends insight to the acquisition process but also provides a relatively simple yet useful tool to aid in solving the experimental design problem. One can quickly test ways of tuning the system so that its response matches the predicted response of the exploration target.

INTRODUCTION

The past few years have seen the emergence of the airgun array as the source of choice for exploration-oriented marine seismology. Airguns are mechanically sound and reliable, are relatively safe and easy to deploy, give a fairly repeatable signal, and can be tuned both temporally and spatially to suit the exploration target. In other words, they are relatively efficient and cost-effective as a seismic source.

In the design and evaluation of such arrays the most commonly used parameters are the peak-to-peak amplitude measure and peak-to-bubble ratio of the far field signature (Giles and Johnston, 1973; Nooteboom, 1978; Johnston, 1982). The first is a measure of source strength. The second is, to some extent, a measure of bandwidth. Unfortunately a simple statement of peak-to-peak gives no indication of the direction in which the energy is transmitted. This can be important, for energy not aimed at the seismic target not only may be wasteful but in fact may generate noise on the seismic section. Similarly, the simple peak-to-bubble ratio is related only rather obscurely to the "whiteness" of the actual signal that reaches a target at some depth in the earth (Larner *et al.*, 1982).

It is the intention of this paper to suggest using a kf domain presentation of the source signature in addition to the more standard displays. This presentation allows for a multifrequency demonstration of array directivity in a single diagram. As well, the presentation can easily incorporate all aspects of system response in such a way that the signature presented is not simply that of the source but is the Fourier domain response of the entire acquisition system.

MODELLING THE kf SYSTEM RESPONSE

The kf presentation will be introduced by taking a particular array as an example. The array consists of four subarrays as shown in Figure 1. Each subarray has eight guns that are fired simultaneously. These range in volume from 40 to 300 cu in, with the total volume of the array being 4520 cu in. The subarrays are towed in an *en echelon* pattern such that the inline length of the array is 43 m. The arrays are deployed with a 25-m crossline separation so that the total width of the array is 75 m.

Figure 2 is a simulated far field signature of the array in time. The signature is derived by simply summing the measured signatures of each of the individual guns in the array directly below the array. This is the most straightforward method of estimating array response, though by no means the most accurate. For a more complete discussion of such estimates the reader is referred to Dragoset (1984), Vaage *et al.* (1983), Parkes *et al.* (1982), or Ziolkowski (1970). The modelled peak-to-peak amplitude of this array is something in excess of one hundred bar-metres. The peak-to-bubble ratio for this array exceeds 10-to-1. The frequency domain representation of this far-field signature (Fig. 3) shows that the effect of the bubble is to cause a ripple on the spectrum within the seismic band. The signature is relatively white from about 10 to 60 Hz. The characteristic notch caused by the surface ghost appears at 97 Hz, as is appropriate for a source depth of 7.6 m (Giles and Johnston, 1973).

[1]Paper presented at the CSEG - GGU National Convention, May 7-10, 1985, Calgary, Alberta, Canada.
[2]Pulsonic Geophysical Ltd., 700, 10201 Southport Rd. S.W., Calgary, Alberta
Far field signature models and polar plots were calculated with a program provided to me by R. Edel, Manager Marine Quality Control, Digicon Geophysical Corp., Houston, Texas.

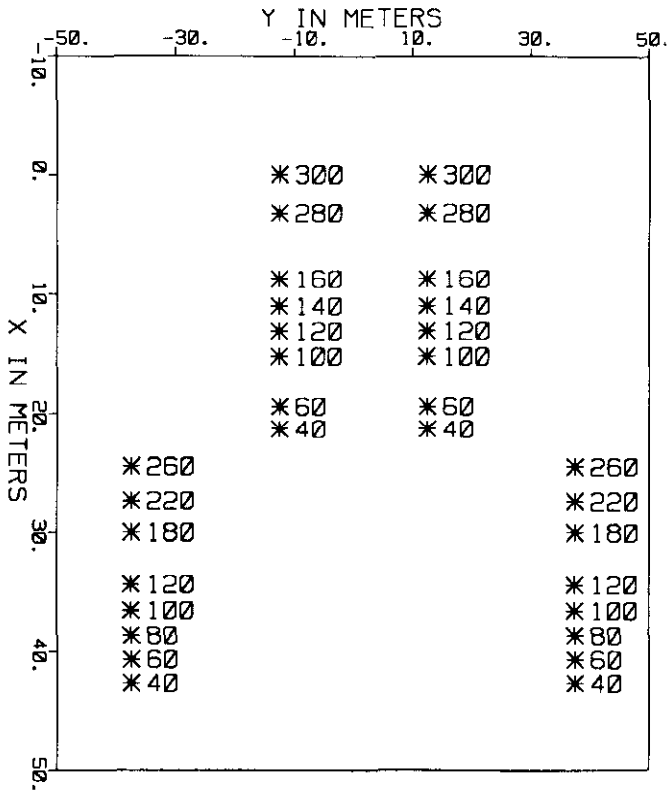

Fig. 1. Diagram showing gun volumes and locations for the 4520-cu-in wide array used as the first example. The ship would be located approximately at (-50,0) while the seismic streamer would begin at about (250,0)

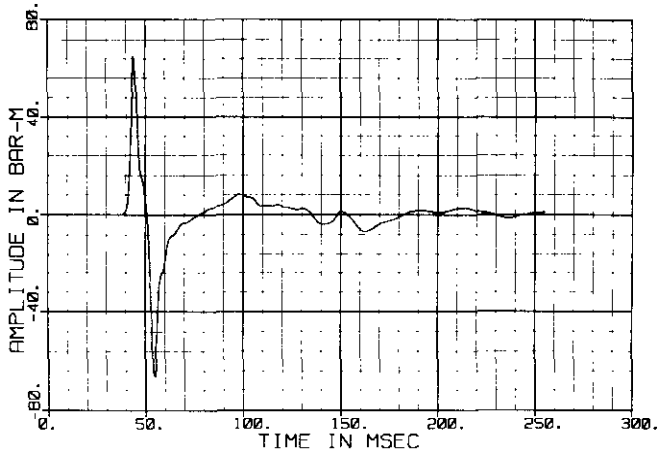

Fig. 2. Simulated far-field time signature of the 4520-cu-in array.

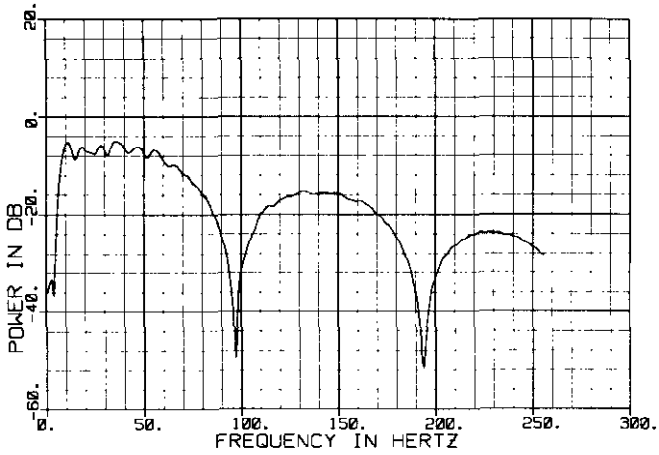

Fig. 3. Power spectrum of the far-field signature of the 4520-cu-in array.

These figures represent the standard way in which one would evaluate this particular array. Figure 4 is an attempt to relate how the energy at 30 Hz is being distributed in space. The angle from the horizontal in degrees is plotted around the outside of this circle, with the boat off to the right. The contours represent, for a single frequency, the amount of power that the array is producing in decibels relative to the peak of its spectrum. At 90 degrees, or straight downward, the array is generating its peak power. At 30 degrees off the vertical, the power is down 6 to 8 dB and becomes progressively less toward the horizontal. The radiation pattern is clearly asymmetric and tilted slightly aft toward the CMPs being sampled. The 40-Hz radiation pattern in Figure 5 demonstrates the result of destructive interference between the various signals. Again, most of the energy is being directed back toward the cable.

Such diagrams are fairly useful, though a little bit cumbersome in that they illustrate only one frequency at a time. Let us now progress to the kf representation, which will provide directional information over a wide band as well as some idea of source strength in a single diagram.

Figure 6 is the inline kf far-field representation of the signature for the 4520-cu-in array. Ghost and group response operators have not been included. The diagram results from a simple two-dimensional Fourier transform of the three-dimensional array that completely describes the source (see Fig. 7). Transformation has been performed on the x (inline position) and t co-ordinates of the array, ignoring the crossline offsets (y co-ordinates) of the guns. This gives a result in $k_x f$ space valid for $k_y = 0$. The result is approximately valid for all k_y when the width of the array is small compared with the wavelengths observed. Positive wavenumbers represent the increasing offset direction of wave travel. Negative wavenumbers represent energy that is propagating back up the cable. The power in dB relative to peak that the array is transmitting as a function of frequency at various wavenumbers is contoured at 12-dB intervals. Signal that is travelling with a horizontal wave front will plot on the vertical axis. The implication of this diagram is that most of the energy from this array is being directed downward. It should be noted that a similar procedure could be used to obtain the cross line (k_y) characteristics of the array. For a complete analysis, the full-blown three-dimensional transform could be performed.

Now consider some of the other factors that the acquisition system encounters. In Figure 8, the gun

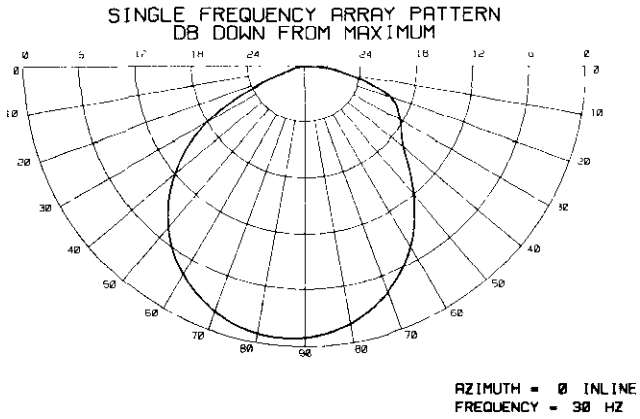

Fig. 4. Polar plot of the in-line radiation pattern at 30 Hz for the 4520-cu-in array. The array orientation is assumed with the ship off to the right and the cable to the left.

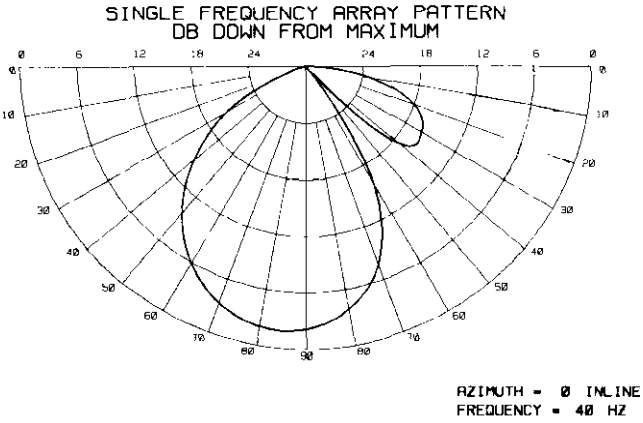

Fig. 5. Polar plot of the in-line radiation pattern at 40 Hz for the 4520-cu-in array. The array orientation is as in Figure 4.

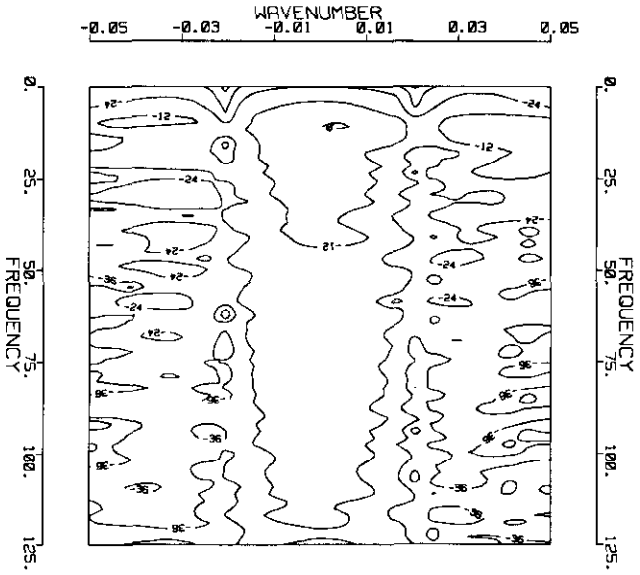

Fig. 6. Kf domain plot of the gun signature for the 4520-cu-in array. Ghosting and cable group response are not included. Contour interval is 12 dB. Positive wave numbers represent waves travelling in the positive x direction.

ghost has been added in. As before it produces a notch at about 97 Hz and multiples of 97 Hz. This notch is identified quite clearly along the zero wavenumber axis. What the previous diagram couldn't show is that the ghost notch is offset-dependent. At lower apparent velocities the ghost notch moves to higher frequencies. This produces a chevron pattern in the contours.

In Figure 9 the wavenumber response of the cable group has been included. (Schoenberger, 1970). This is a 25-m, 14-phone group which will respond with its first zero in wavenumber space at 0.04 m^{-1}. The notches in the spectrum introduced by the response of the cable group are evident in the figure. The cable will also have a ghost, the effect of the water surface reflection on its response. Figure 10 incorporates the ghost operator for a 10-m cable depth. This has the effect of introducing a second notch at about 74 Hz. Again this is offset-dependent, so the effect moves to higher frequencies at higher wavenumbers.

The last figure represents the entire system response of the marine acquisition system, except perhaps for instrument filters. What possible use can be made of these? Perhaps one can compare one system with another, using not only the common far-field signature diagrams, but also the kf representation.

Using the Model for Array Selection

Figure 11 is a cartoon of the three arrays to be compared. The result for array A, where the four subarrays are towed in a chevron pattern that is about 40 m long, has already been shown. Next, the result of towing four arrays abreast so that the total length of the array is 20 m, will be given and, finally, that for an array over 300 m in length will be discussed.

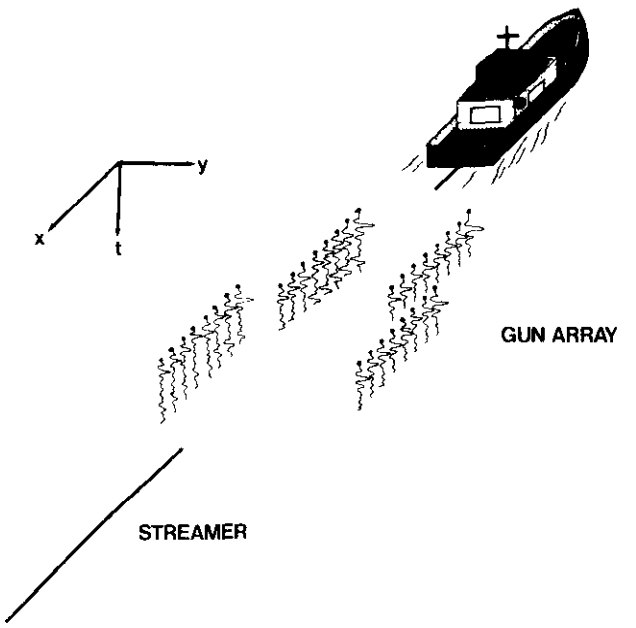

Fig. 7. Schematic diagram to illustrate layout of array in (x,y,t) space. Fourier transforms of the x and t co-ordinates are performed to derive the kf diagrams presented.

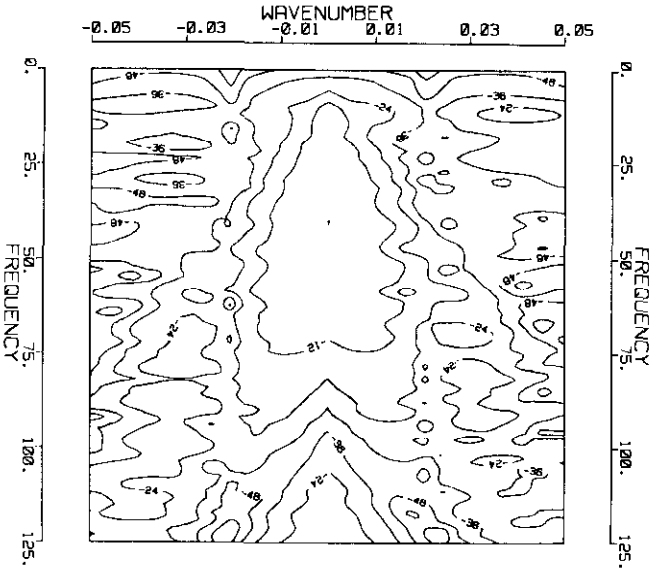

Fig. 8. Kf domain plot of the ghosted gun signature for the 4520-cu-in array.

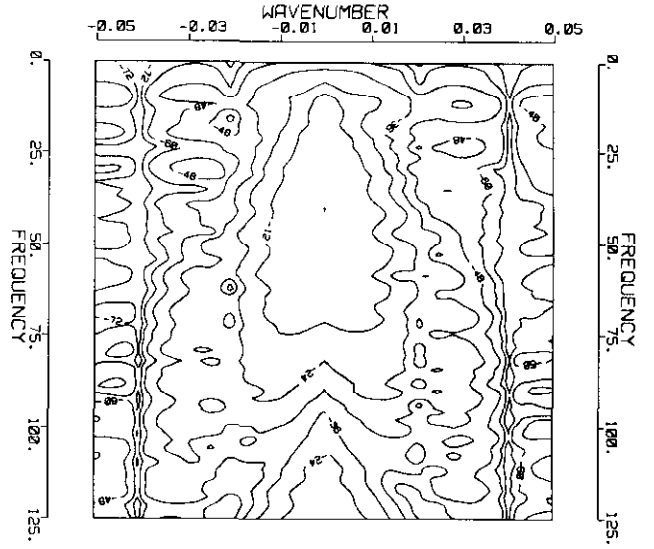

Fig. 9. Kf domain plot of the ghosted gun signature for the 4520-cu-in array with the response of a 25-m, 14-phone, unweighted hydrophone group included.

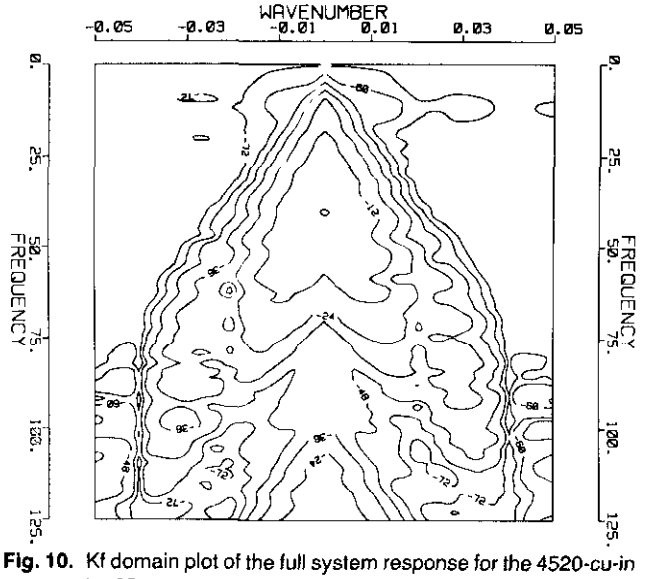

Fig. 10. Kf domain plot of the full system response for the 4520-cu-in array and a 25-m group. Gun and cable ghosts are included.

Figure 12 illustrates the configuration where the subarrays are towed parallel and abreast. The modelled far-field time signature is given in Figure 13. The peak-to-peak amplitude for this array, at close to 120 bar-metres, is a little larger than for the previous array because the total volume is 5000 cu in. The peak-to-bubble ratio is smaller because the bubble pulse at around 100 ms after the initial pulse is slightly larger than previously. The effect of this can be seen in Figure 14, which is just the power spectrum of the signal. The poor peak-to-bubble ratio translates into deeper notches within the seismic band. In Figure 15 the kf representation of the entire system is displayed. Again one can see the prevalent effect of the cable and source ghost, the limiting wavenumber notch for the cable group response, and the over-all distribution of transmitted energy. The focusing mechanism of the array is still active, but not so effectively as before. Slower apparent velocities are being excited because the array is shorter. We will now look at the long array and see if our arguments hold true.

Figure 16 displays the set-up of the 300-m-long array. The array is made up of 40 identical 80-cu-in guns spaced at about 8 m along a string. The total volume is 3200 cu in. These guns are identical, so their bubbles reinforce each other rather than interfering destructively; therefore a very poor peak-to-bubble ratio is to be expected. This is borne out in both the time response (Fig. 17) and the power spectrum (Fig. 18). The peak-to-peak amplitude is quite a bit smaller than in the previous arrays, because the total volume of the gun system is only 3200 cu in. The peak-to-bubble ratio is only about 1. On the power spectrum (Fig. 18) this peak-to-bubble ratio results in notches within the seismic band that are very deep. This is not a very attractive spectrum from the point of view of whiteness within the seismic band.

Moving to the kf domain (Fig. 19), the effect of the length of the array is very apparent. The concentration of energy is distinctly on the zero wave-number axis. This is effectively a plane wave source. Very little energy is transmitted at the low apparent velocities. Very little energy is directed at shallow angles from the horizontal toward the back or the front of the system. As before, the signature shows the two ghost notches and some wave-number band-limiting as a result of the cable group response.

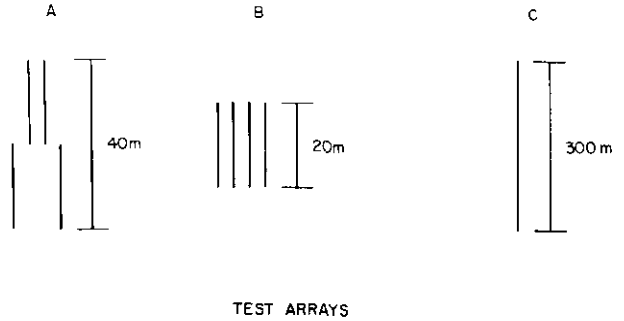

Fig. 11. *Schematic layout of three arrays to be compared. Array A is* the 4520-cu-in example already discussed.

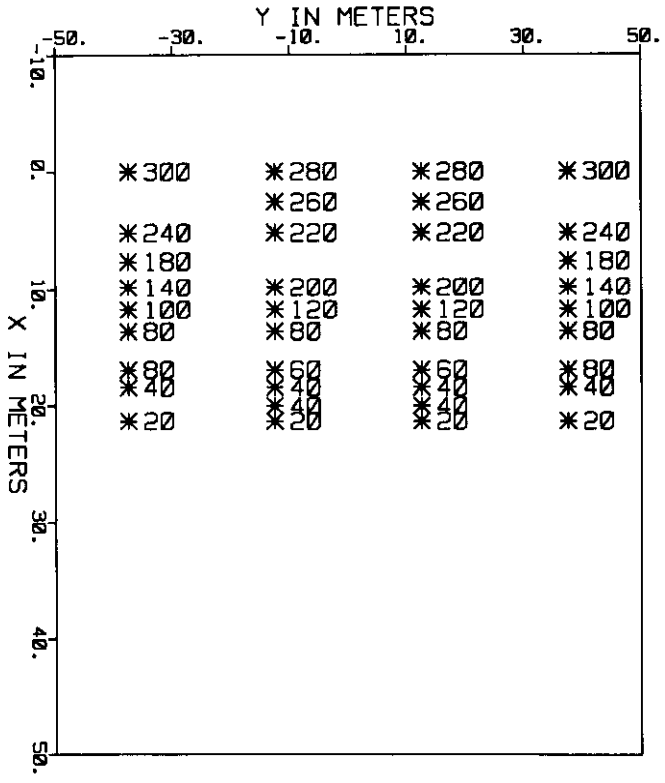

Fig. 12. Gun layout diagram for array B. The towing direction is decreasing x as in Figure 1.

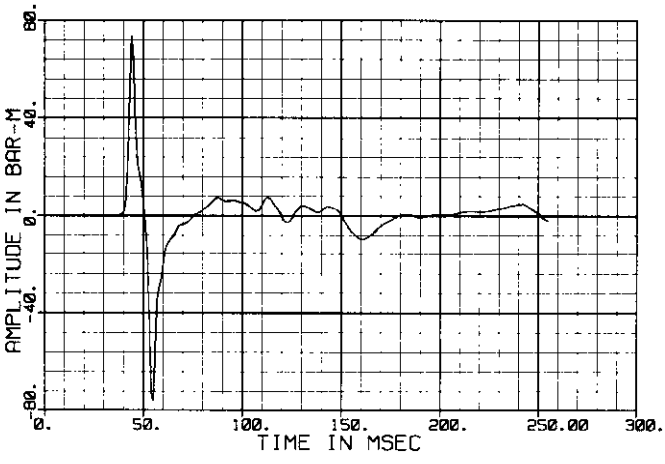

Fig. 13. Modelled far-field time signature of array B.

Clearly, the differences between one array and another can be seen as a result of doing this kind of analysis, but which array is better?

One can, of course, look at some real data from the target area to see what kind of frequencies, spatial and temporal, are characteristic of the area. Figure 20 is data from Canada's east coast presented in kf domain. The source array was in a 40 by 75 m chevron pattern with a total volume of about 4000 cu in. The cable group length and interval were 15 m. Note the 1500 m per second apparent velocity line, the lower limit of any

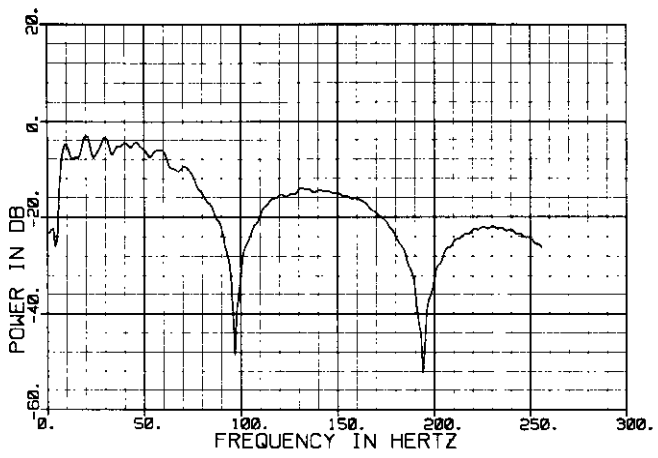

Fig. 14. Power spectrum of far-field signature, array B.

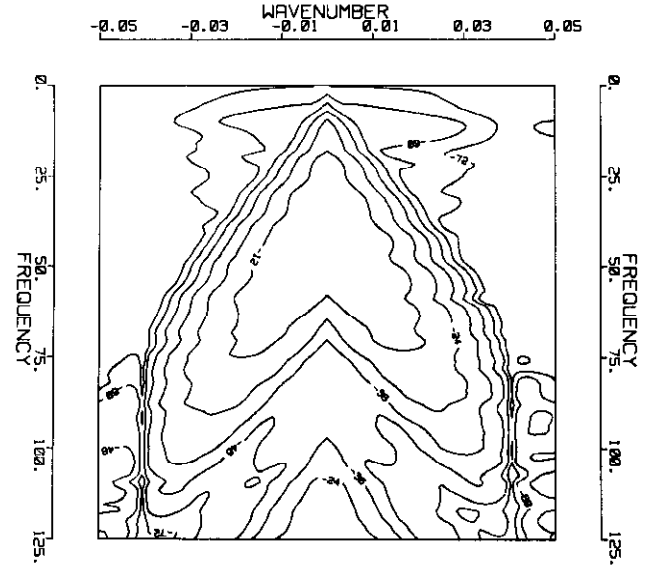

Fig. 15. Kf domain plot of the full system response for array B.

available data. There is some noise evident at about 2500 m/s. The largest part of the reflected energy has an apparent velocity of 4500-5000 m/s. Also notice the aliasing of the slowest data at the higher frequencies. By examining this sort of diagram, one could determine what part of the kf plane the acquisition system should be tuned to (Schoenberger, 1970). Such a study can be useful before returning to shoot in an area, but what if there are no previous data to analyze?

It is possible to estimate the apparent velocities to be expected with rather simple calculations of the form:

$$V_{app} = \frac{t_x V^2}{x + T_o V \sin \phi},$$

where x is the shot-to-receiver offset,
t_x is the event arrival time at offset x,
T_o is the zero-offset vertical incidence arrival time,
ϕ is the dip of the event,
V is the rms velocity.

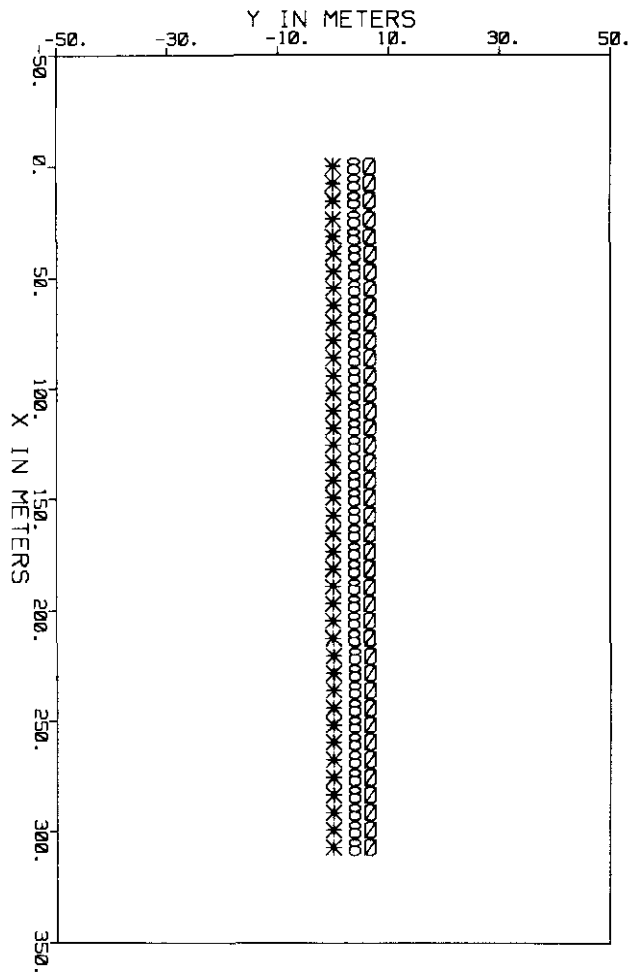

Fig. 16. Gun layout diagram for array C. The towing direction is decreasing x as in Figure 1.

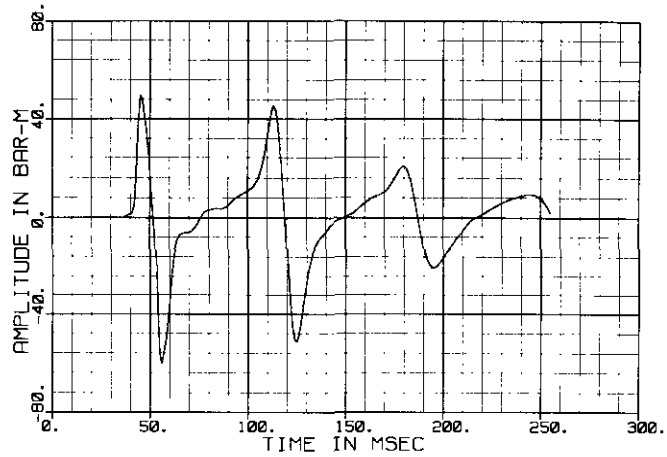

Fig. 17. Modelled far-field time signature, array C.

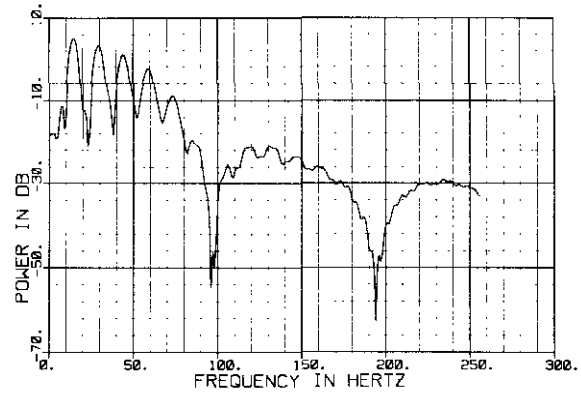

Fig. 18. Power spectrum of far-field signature of array C.

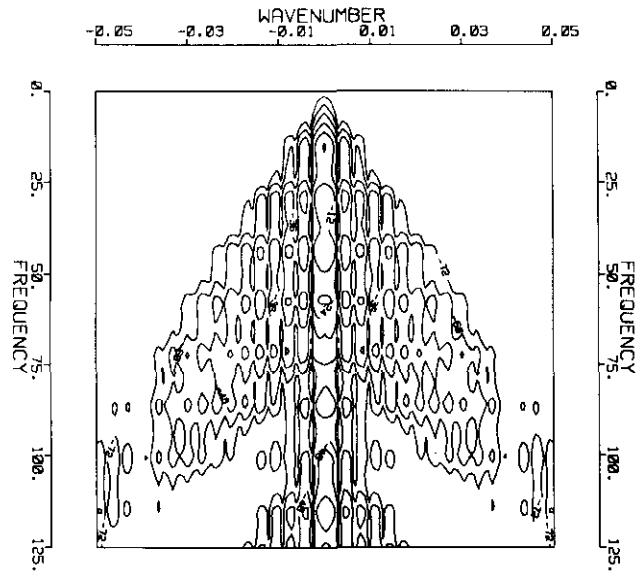

Fig. 19. Kf domain plot of the full system response for array C.

Figure 21 presents a model that consists of four seismic events. The first will be recognized as the water bottom by its velocity. The second, third and fourth are set at 700, 1300 and 2800 ms two-way time and 1870, 2000 and 2800 m/s rms velocity. Figure 22 presents the apparent velocities as a function of offset calculated for reflections from these events. The apparent velocity of the water-bottom multiple has also been included. In this manner the apparent velocities of the key events can be predicted. This in turn indicates what part of the kf plane needs to be sampled by the system. Returning to the model example, let us assume we will limit this experiment to apparent velocities of 3000 m/s and faster. By doing this nothing is lost, in terms of the modelled objectives, out to offsets of 2000-3000 m. Most of the water bottom is not imaged, but this is usually not a problem. If 3000 m/s is accepted as a good lower limit to the apparent velocities that should be retained, then the target band for system response is as pictured in Figure 23.

How do the three arrays modelled compare with this target? Figures 24, 25 and 26 are replots of the kf response of the chevron (array A), four-abreast (array B) and long (array C) arrays with the target zone superimposed. Clearly, array B is best suited to this particular exploration requirement.

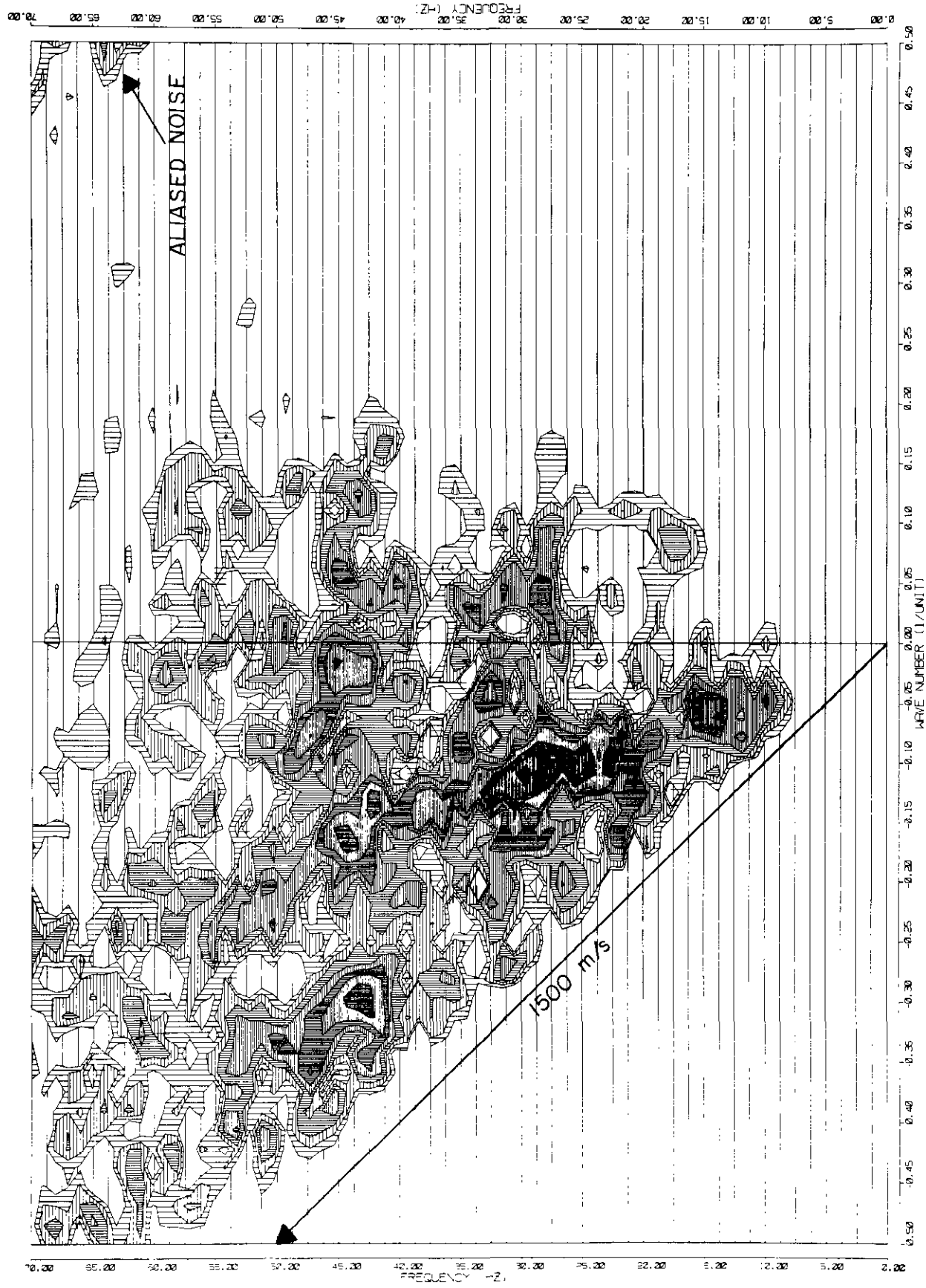

Fig. 20. Kf domain plot of real data from a marine survey. The 1500 m/s apparent velocity line is identified. Noise slightly faster than this (2000-3000 m/s) is evident and aliased. The signal appears strongest in the range 4500-5000 m/s. The contour interval is 3 dB.

SEISMIC MODEL

EVENT 1	To = 100 msec	Vs = 1470 m/s
EVENT 3	To = 700 msec	Vs = 1870 m/s
EVENT 4	To = 1300 msec	Vs = 2000 m/s
EVENT 5	To = 2800 msec	Vs = 2800 m/s

Fig. 21. Simple layered earth model used to calculate apparent velocities to be expected in data.

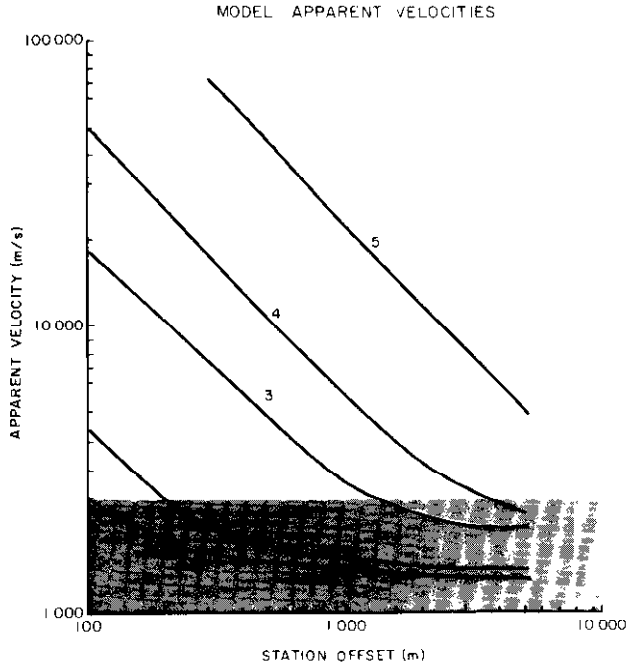

Fig. 22. Plot of the apparent velocities as a function of offset to be expected from the events shown in Figure 20. Event 2 is the water-bottom multiple.

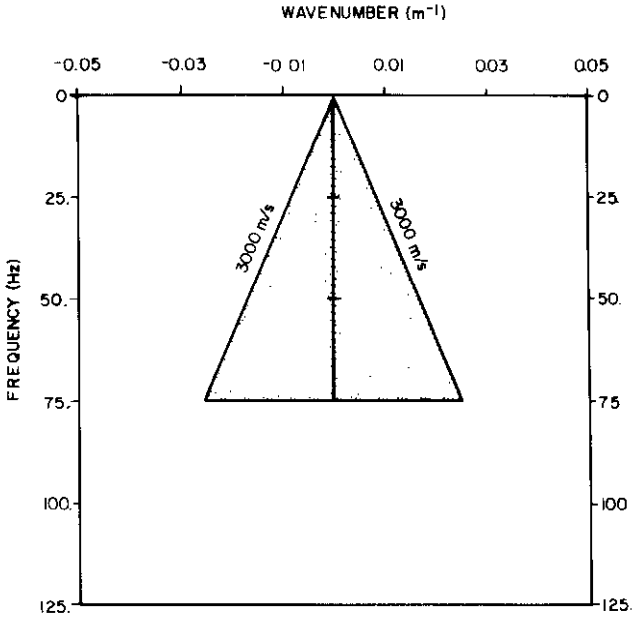

Fig. 23. Target band to be sampled by the acquisition system.

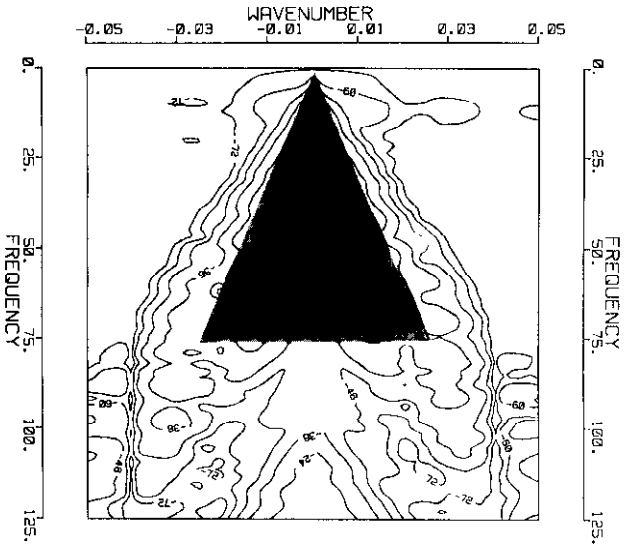

Fig. 24. Comparing the target band with the system response of array A.

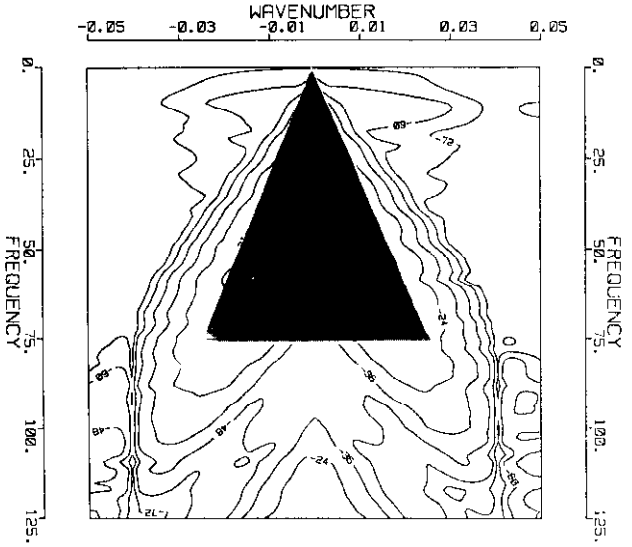

Fig. 25. Comparing the target band with the system response of array B.

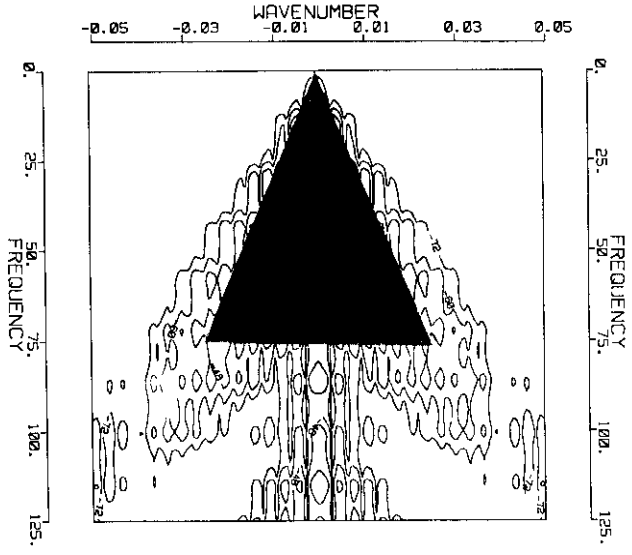

Fig. 26. Comparing the target band with the system response of array C.

CONCLUSION

What this paper presents is not some new and astounding mathematical tool which breaks open the acquisition business, but rather an application of a tried and true analysis technique to a familiar problem. A data presentation is obtained that graphically illustrates the important properties of not only the seismic source but the entire acquisition system. A proper consideration of the exploration target should make it possible to use this kind of presentation to design a more appropriate acquisition system and, hopefully, to acquire better data.

REFERENCES

Dragoset, W. H., 1984, A comprehensive method for evaluating the design of air guns and airgun arrays: The Leading Edge, Oct, p. 52-61.

Giles, B. F. and Johnston, R. C., 1973, System approach to airgun array design: Geophysical Prospecting, v. 21, p. 77-101.

Johnston, R. C., 1982, Development of more efficient airgun arrays: theory and experiment: Geophysical Prospecting, v. 30, p. 752-773.

Larner, K., Hale, D., Zinkhan, S. M. and Hewlitt, C., 1982, Desired seismic characteristics of an airgun source: Geophysics, v. 47, p. 1273-1284.

Nooteboom, J. J., 1978, Signature and amplitude of linear airgun arrays: Geophysical Prospecting, v. 26, p. 194-201.

Parkes, G. E., Ziolkowski, A., Hatton, L. and Haugland, T., 1982, The signature of an airgun array: computation from near field measurements including interactions - practical considerations: Paper presented at 44th annual meeting of the European Association of Exploration Geophysicists, Cannes, France.

Schoenberger, M., 1970, Optimization and implementation of marine seismic arrays: Geophysics, v. 35, p. 1038-1053.

Vaage, S., Haugland, K. and Letheim, T., 1983, Signatures from single airguns: Geophysical Prospecting, v. 31, p. 87-97.

Ziolkowski, A., 1970, A method for calculating the output pressure wave form from an air gun: Geophysical Journal, Royal Astronomical Society, v. 21, p. 137-161.